Computer Simulations of Trypanosomal Nucleoside Hydrolase: Determination of the Protonation State of the Bound Transition-State Analogue

Devleena Mazumder, Kalju Kahn, and Thomas C. Bruice*

Contribution from the Department of Chemistry and Biochemistry, University of California, Santa Barbara, Santa Barbara, California 93106

Received February 28, 2002

Abstract: Inosine-uridine nucleoside hydrolase (IU-NH) catalyzes the hydrolysis of nucleosides into base and ribose moieties via a ribooxocarbenium ion transition state, which has been characterized using kinetic isotope effects. Protozoan parasites lack de novo purine and pyrimidine biosynthesis and depend on the purine salvage from the host. Vern Schramm and co-workers characterized *p*-aminophenyliminoribitol (pAPIR) to be a potent inhibitor of IU-NH from *Crithidia fasciculata* with K_d of 30 nM. The cyclic amine function of the iminoribitol ring can be either protonated (pAPIRH$^+$) or unprotonated (pAPIR). pAPIRH$^+$ resembles the charge and geometry of the ribooxocarbenium ion transition state and can be looked upon as a transition-state analogue inhibitor; however, it is known that the pAPIR species is initially bound to the enzyme. We have characterized the pAPIRH$^+$ species as resident of the active site using ab initio calculations and molecular dynamics simulations. This is a novel use of molecular dynamics to investigate the protonation state of the bound ligand to the active site. Nanosecond molecular dynamics simulations reveal a short hydrogen-bonding network between pAPIRH$^+$-O2′-Asp14-His241 triad, which is not seen in the crystal structure. Other features discussed are: hydrogen bonding between pAPIRH$^+$ and Asn168, unusual geometry of the iminoribitol ring, and hydrophobic interactions.

Introduction

Infectious parasitic diseases such as malaria, African trypanosomiasis, leishmaniasis, and Chagas disease, threaten the majority of the global rural population. Malaria alone is responsible for more than 1 million deaths per year.[1] Vaccines using antibody-based strategies have not proven to be effective because the parasites modify surface glycoproteins to invade the immune system of the host.[2,3] There has been a great deal of interest in designing and developing inhibitors of protozoan nucleoside hydrolase as potential chemotherapeutic agents because no nucleoside hydrolase activity or genes encoding this enzyme have been identified in mammals.[4] These protozoans have developed complex host purine salvage machinery because they lack de novo biosynthetic pathways for purines.[5] Nucleoside hydrolase catalyses the *N*-ribohydrolysis reaction (Scheme 1) and plays a crucial role in the purine salvage from the host DNA and RNA. Understanding the mode of binding of inhibitors and participation of important active-site residues during the inhibition will be useful in the development of drugs for combating these parasitic diseases.

The inosine-uridine nucleoside hydrolase from *Crithidia fasciculata* is a homotetramer of M_r 34 000 subunits.[6] The kinetic mechanism is rapid equilibrium random with respect to product release.[7] Using multiple kinetic isotope effects, Horenstein et al. showed the chemical mechanism to be S_N1-like, which proceeds via an exploded ribooxocarbenium ion transition state with weak bonds to the departing hypoxanthine and incipient water nucleophile.[8] Schramm and co-workers identified *p*-aminophenyliminoribitol (pAPIR) (Chart 1) to be a potent inhibitor for inosine-uridine nucleoside hydrolase (IU-NH) from *C. fasciculata* with K_d of 30 nM.[9] Three-dimensional structures of the free (PDB ID: 1MAS)[6] and the inhibitor bound (PDB ID: 2MAS)[10] have been determined recently by X-ray crystallography. The protonation state of the bound inhibitor is uncertain because the cyclic amine function (pK_a 6.5) of the iminoribitol ring can be either protonated (pAPIRH$^+$) or unprotonated (pAPIR).[11] The pH analysis of the binding of phenyliminoribitol inhibitor supports the neutral inhibitor as the species that binds to the enzyme.[7,9,11,12] However, analysis of

---

* To whom correspondence should be addressed. Telephone: 805-893-2044. Fax: 805-893-2229. E-mail: tcbruice@bioorganic.ucsb.edu.

(1) WHO Fact Sheet, No. 94; World Health Organization: New York, 1998.
(2) Cross, G. A. M. *Parasitology* **1975**, *71*, 393.
(3) Vickerman, K. *Br. Med. Bull.* **1985**, *41*, 105.
(4) Gopaul, D. N.; Meyer, S. L.; Degano, M.; Sacchettini, J. C.; Schramm, V. L. *Biochemistry* **1996**, *35*, 5963.
(5) Hammon, D. J.; Gutteridge, W. E. *Mol. Biochem. Parasitol.* **1984**, *13*, 243.

(6) Degano, M.; Gopaul, D. N.; Scapin, G.; Schramm, V. L.; Sacchettini, J. C. *Biochemistry* **1996**, *35*, 5971.
(7) Parkin, D. W.; Horenstein, B. A.; Abdulah, D. R.; Estupiñán, B.; Schramm, V. L. *J. Biol. Chem.* **1991**, *266*, 20658.
(8) Horenstein, B. A.; Parkin, D. W.; Estupiñán, B.; Schramm, V. L. *Biochemistry* **1991**, *30*, 10788.
(9) Parkin, D. W.; Limberg, G.; Tyler, P. C.; Furneaux, R. H.; Chen, X.-Y.; Schramm, V. L. *Biochemistry* **1997**, *36*, 3528.
(10) Degano, M.; Almo, S. C.; Sacchettini, J. C.; Schramm, V. L. *Biochemistry* **1998**, *37*, 6277.
(11) Horenstein, B. A.; Schramm, V. L. *Biochemistry* **1993**, *32*, 9917.
(12) Parkin, D. W.; Schramm, V. L. *Biochemistry* **1995**, *34*, 13961.
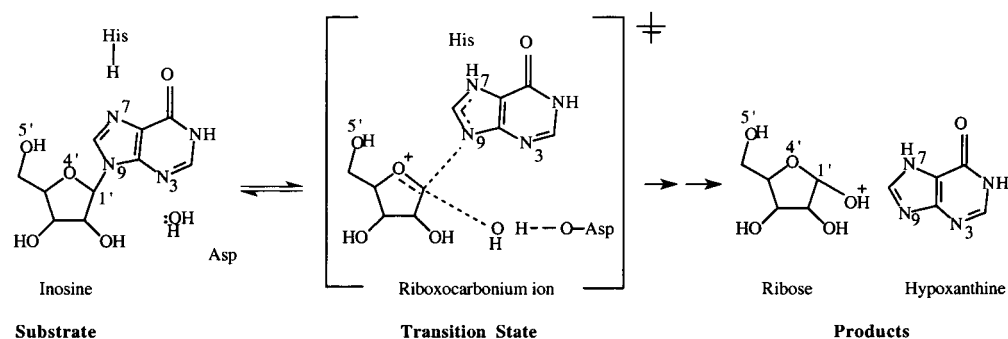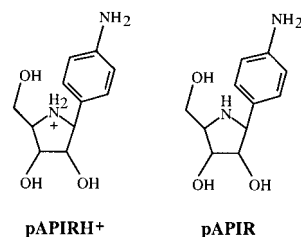
Scheme 1

Chart 1

the slow-onset component of inhibition suggested that the neutral form may be subsequently protonated in the enzyme active site.[12]

We employed ab initio calculations and molecular dynamics (MD) simulations of both Enzyme·pAPIR and Enzyme·pAPIRH⁺ complexes to establish the protonation state of the bound inhibitor and to explore the dynamic structure of the enzyme−inhibitor complex.

Methods

MD Setup. The starting coordinates of the inhibitor-bound *Crithidia fasciculata* nucleoside hydrolase homotetramer (314 amino acid residues in each subunit) were taken from the entry 2MAS in the Protein Data Bank. Hydrogen atoms were added to the X-ray structure via the empirical energy placement protocol H-BUILD[13] in the CHARMM program.[14] Aspartate, glutamate, arginine, and lysine residues were charged, and all the tyrosine residues were neutral. The protonation sites of histidine residues were based on the availability of H-bond donors or acceptors nearby. Mutation studies provided the evidence that the active-site histidine, His241, is the general acid, which protonates the leaving group of the substrate.[4] On the basis of this evidence, His241 was protonated on both N-ϵ and N-δ sites. Partial atomic charges for the inhibitor and the active-site Thr126 in the presence of calcium cation were obtained as described later.

The enzyme−inhibitor system was solvated in an equilibrated TIP3P water sphere of 42 Å radius using the center of mass of the inhibitor as the origin (Figure 1). Stochastic boundary molecular dynamics (SBMD)[15] was carried out on the active-site region of the subunit D using the CHARMM force field.[14] The solvated system contained the whole of subunit D with inhibitor and the calcium ion bound to the active site, and included parts of A, B, and C subunits.

Any solvent molecule within 2.8 Å of a heavy atom of the enzyme or crystallographic water molecule was deleted. The 6508 added solvent molecules (19524 atoms) were minimized and equilibrated at 300 K for 3 ps, keeping the protein, inhibitor, and the crystallographic water molecules fixed to allow favorable distribution of water molecules on the enzyme surface. For SBMD, we used 40 Å reaction zone with 2 Å
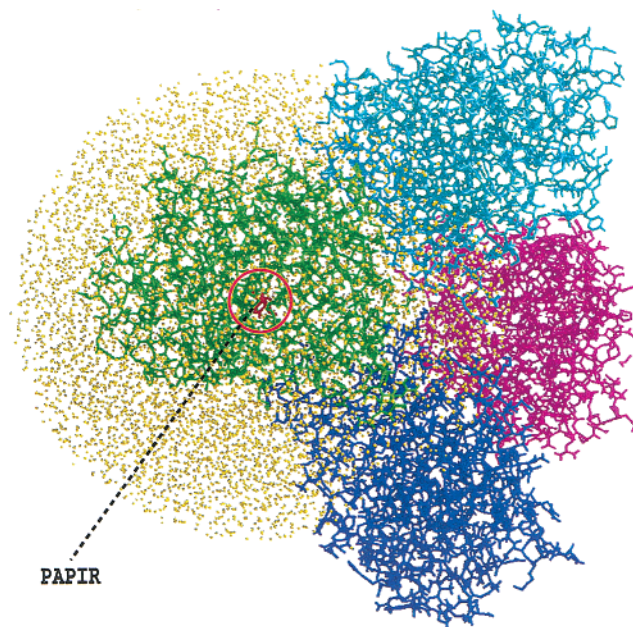
(13) Brunger, A. T.; Karplus, M. *Proteins* **1988**, *4*, 148.
(14) Brooks, B. R.; Bruccoleri, R. E.; Olafson, B. D.; States, D. J.; Swaminathan, S.; Karplus, M. *J. Comput. Chem.* **1983**, *4*, 187.
(15) Brooks, C. L., III; Karplus, M. *J. Mol. Biol.* **1989**, *208*, 159.

Figure 1. Stochastic boundary molecular dynamics setup for the enzyme−inhibitor system using 42 Å TIP3P water sphere. Four subunits are shown in different colors. The inhibitor bound to the active site is circled in red.

buffer region. All the protein atoms that were at a distance further than 42 Å from the center of mass were deleted after the minimization. Eleven sodium ions were added to maintain the electroneutrality of the system. Both Enzyme·pAPIR and Enzyme·pAPIRH⁺ models contained a total of ∼30 300 atoms (10 410 atoms of enzyme, 1 calcium atom, 32 (neutral)/33 (protonated) atoms of inhibitor, 11 sodium atoms, 90 crystallographic water molecules). The same protocols for energy minimization and dynamics were used for both models. Before the start of the dynamics, the enzyme−inhibitor systems were energy minimized using the steepest descents (SD) method followed by the adopted basis Newton−Raphson (ABNR) method for 5000 steps.[14] Because the numbers of atoms in both systems are rather high, extensive energy minimizations were carried out to obtain suitable starting structures for the molecular dynamic studies. The CHARMM 27 residue topology and parameter file were used for protein atoms and the inhibitor. The system was coupled to a heat bath of 300 K using a frictional coefficient of 250 ps⁻¹ on the heavy atoms of the enzyme. All buffer region water oxygens were assigned a frictional coefficient of 62 ps⁻¹. Heavy atoms of the protein in the buffer region were constrained using force constants calculated from their average Debye−Waller factors.[15] Bonds containing hydrogen were constrained using SHAKE algorithm.[16] Molecular dynamics using constant pressure and temperature were done for both models for 1 ns using an integration time step of 0.001 ps.

(16) Ryckaert, J. P.; Ciccotti, G.; Berendsen, H. J. C. *J. Comput. Phys.* **1977**, *23*, 327.

Chart 2
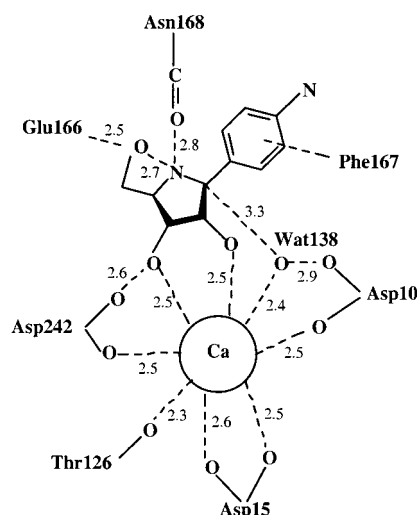
The X-ray crystal structure places a nucleophilic water molecule Wat138 in position to occupy one of the coordination sites of the octacoordinated calcium ion and at 3.3 Å from the ribosyl 1′-carbon of pAPIR in subunit D (Chart 2). Preliminary simulation results showed that this water molecule does not exchange with waters from the water pool. However, the calcium−water distance increased from 2.48 to 4 Å during the test dynamics. Thus, a distance constraint was placed between the active-site nucleophilic water and calcium ion using a large force constant of 10 000. Both the 2′- and 3′-hydroxyl oxygen of pAPIRH$^+$ (SBMD1) remained bound to the active-site calcium, but it was difficult to keep the neutral inhibitor (pAPIR) bound to the active site without some distance constraints. During a test simulation, the 2′- and 3′-hydroxyls of pAPIR were found to fall apart from calcium and the active site and relocate to a different region next to the active site. For this reason, the MD on the neutral inhibitor was carried out using a small force constant on the oxygen to calcium distance ($R_{Ca\cdots O2}$ = 2.5 Å, force constant = 10; $R_{Ca\cdots O3}$ = 2.5 Å, force constant = 10). The molecular dynamics results and statistical analysis were carried out for the last 815 ps of both the simulations. Covariance matrix was used to determine the extent of correlated motion between the α-carbons of the residues. For all our calculations, only the D-subunit was considered. Preliminary calculations were carried out on an SGI Indigo 2 workstation, and molecular dynamics simulations were performed on a SGI platform at the Origin2000, UCSB Supercomputing Center.

Reassignment of Partial Charges on the Basis of ab Initio/RESP Calculations. Lennard-Jones (LJ) parameters for the calcium ion developed by Marchand and Roux (1998) were used for our MD simulation.[17] The protein and inhibitor were described by the standard CHARMM27 parameters except as noted below. The X-ray crystal structure of the enzyme−inhibitor complex showed that the calcium ion in *C. fasciculata* nucleoside hydrolase is octacoordinated, which includes coordination by the active-site aspartate residues (Asp10 OD1, Asp15 OD1 and OD2, Asp242 OD2), water (Wat138), backbone carbonyl oxygen (O) of Thr126, and the 2′- and 3′-oxygen of the inhibitor. Test simulations suggested a need to reparametrize atomic charges of backbone carbonyl of Thr126 and hydroxyls of inhibitor to account for the charge polarization by Ca^{2+}. Since the charge distribution allotted to the backbone carbonyl and hydroxyl group in the CHARMM parameter file was not calculated in the close proximity of a cation, it was reasonable to assume that the backbone carbonyl and the inhibitor hydroxyls in our model should be more polarized. Partial atomic charges were determined by fitting point charges to the molecular electrostatic potential. Acetamide, which was used as a model compound for the peptide bond of Thr126, was optimized at the MP2/

6-31+G(d,p) level of theory. Single-point calculations of Ca^{2+}-acetamide complex were performed by varying the oxygen−calcium distances from 1.8 to 10.0 Å. The electrostatic potentials at these points were obtained from the MP2/6-311+G(2d,p) density using the Merz−Kollman scheme implemented in Gaussian98.[18] RESP fitting[18,19] of point charges to these electrostatic potentials was done to obtain charges for the model compound. On the basis of our MP2/RESP calculation, the charge of the carbon of Thr126 was changed from 0.5 eu to 0.7 eu. Similarly, the partial charge of the Thr126 carbonyl oxygen atom was changed from −0.5 eu to −0.7 eu.

A similar approach was followed for the charge calculations of the inhibitor 2′- and 3′-hydroxyl group in the presence of calcium ion. 2-Propanol was used to model hydroxyl groups of the inhibitor. The charges obtained by MP2/RESP calculations of the 2-propanol−calcium ion complex were averaged over the distance 2 to 2.4 Å to give a more representative charge distribution for the MD simulation. The following changes in the charges were made: C2 (0.14 → 0.44), O2 (−0.66 → −0.96), H2 (0.43 → 0.63). The new charges were tested by calculating an interaction energy profile in the 2-propanol−calcium ion complex at various oxygen−Ca^{2+} distances (1.6 to 20.0 Å) using MP2/6-31+G-(d,p) level of theory. The basis set superposition error (BSSE)[20] was corrected by the counterpoise method.[21] It was found that the interaction energy as predicted using CHARMM charges was about 17% less than that predicted by MP2/RESP. All the ab initio calculations were done using GAUSSIAN 98.[22]

Ab Initio Conformational Analysis of the Inhibitor. The protonation state of the imino group of the enzyme-bound ligand was investigated by optimizing the structures of the protonated and neutral models of the inhibitor at the MP2/6-311+G(d,p) level. Three structural models with different degrees of substitution in the iminoribitol ring were considered. First, conformational analyses of the 5′-hydroxyl group in the neutral and protonated 2′,3′-dideoxyiminoribitol were performed by considering the anti and the two gauche orientations of the 5′-hydroxyl group. Then, conformational analysis of 2′-deoxyiminoribitol was performed followed by minimization of one of the low-energy conformers of iminoribitol. Starting structures for neutral models had the 5′-hydroxyl group in the gauche$^-$ orientation because this orientation was found to be the global energy minimum in 2′,3′-dideoxyiminoribitol. For a similar reason, the 5′-hydroxyl group in protonated models was in the anti orientation. The 3′-hydroxyl group was in the gauche$^-$ orientation (relative to the C4′ atom of the iminoribitol ring) in all molecules. These ab initio optimized structures were compared to the crystal structure of the bound inhibitor.

Results

Results from Molecular Dynamics Simulations. Comparison of MD and X-ray Structure. Molecular dynamics simulations of nucleoside hydrolase were performed with the protonated (SBMD1) and neutral (SBMD2) inhibitor. Both simulations produced stable root-mean-squared deviations (RMSD) for the

(17) Marchand, S.; Roux, B. *Proteins: Struct., Funct., Genet.* **1998**, *33*, 265.

(18) Besler, B. H.; Merz, K. M. J.; Kollman, P. A. *J. Comput. Chem.* **1990**, *11*, 431.
(19) Bayly, C. I.; Cieplak, P.; Cornell, W. D.; Kollman, P. A. *J. Phys. Chem.* **1993**, *97*, 10269.
(20) Ransil, B. J. *J. Chem. Phys.* **1961**, *34*, 2109.
(21) Boys, S. F.; Bernardi, F. *Mol. Phys.* **1970**, *19*, 553.
(22) Frisch, M. J.; Trucks, G. W.; Schlegel, H. B.; Scuseria, G. E.; Robb, M. A.; Cheeseman, J. R.; Zakrzewski, V. G.; Montgomery, J. A.; Stratmann, R. E.; Burant, J. C.; Dapprich, S.; Millam, J. M.; Daniels, A. D.; Kudin, K. N.; Strain, M. C.; Farkas, O.; Tomasi, J.; Barone, V.; Cossi, M.; Cammi, R.; Mennucci, B.; Pomelli, C.; Adamo, C.; Clifford, S.; Ochterski, J.; Petersson, G. A.; Ayala, P. Y.; Cui, Q.; Morokuma, K.; Malick, D. K.; Rabuck, A. D.; Raghavachari, K.; Foresman, J. B.; Cioslowski, J.; Ortiz, J. V.; Stefanov, B. B.; Liu, G.; Liashenko, A.; Piskorz, P.; Komaromi, I.; Gomperts, R.; Martin, R. L.; Fox, D. J.; Keith, T.; Al-Laham, M. A.; Peng, C. Y.; Nanayakkara, A.; Gonzalez, C.; Challacombe, M.; Gill, P. M. W.; Johnson, B.; Chen, W.; Wong, M. W.; Andres, J. L.; Gonzalez, C.; Head-Gordon, M.; Replogle, E. S.; Pople, J. A. *Gaussian 98*; Gaussian, Inc.: Pittsburgh, PA, 1998.
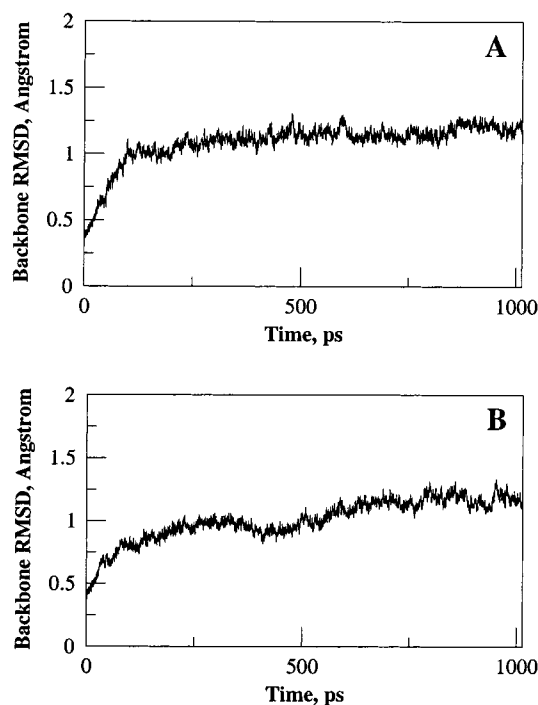
Figure 2. Root-mean-squared deviation of the D-subunit from SBMD1 (A) and SBMD2 (B).
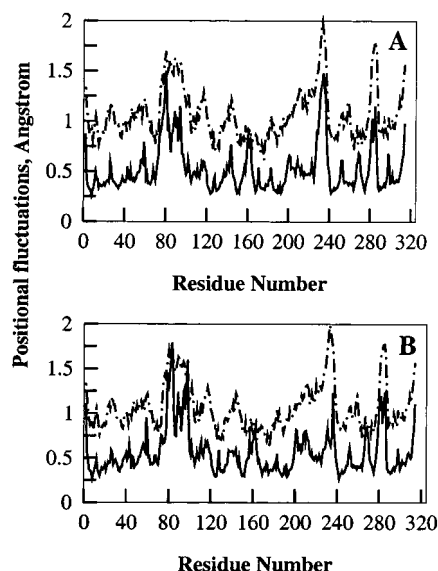

Figure 3. (A) Positional fluctuations for the α-carbons of the D-subunit during production phase in SBMD1 (solid line) and *B*-factors from X-ray crystal structure (dotted line). (B) Positional fluctuations for the α-carbons of the D-subunit during production phase in SBMD2 (solid line) and *B*-factors from X-ray crystal structure (dotted line).

protein backbone (excluding calcium ion and hydrogen atoms) after the first 150 ps (Figure 2). The RMSD for SBMD1 and SBMD2 averaged at 1.08 ± 0.16 and 1.02 ± 0.17 Å, respectively. Positional fluctuations for the Cα atoms of D-subunit from SBMD1 and SBMD2 were compared with crystallographic *B*-factors, and a good agreement was found (Figure 3). Slight deviations from the experimental structure were observed for the calcium−ligand distances and are localized only to the nearest neighbors of calcium ion. The results obtained about the important features of inhibitor binding from the MD simulations are discussed in the following sections.

Enzymatic Contacts with the Iminoribitol Ring of pA-PIRH$^+$ (SBMD1). The average calcium-to-oxygen distances of the amino acids ligated to the octacoordinated calcium ion were close to that provided by X-ray: backbone carbonyl of Thr126 (2.2 ± 0.06 Å), bidentate Asp15 (2.3 ± 0.1, 2.2 ± 0.07 Å), Asp242 (2.2 ± 0.06 Å), and Asp10 (2.2 ± 0.06 Å). These bond distances were found to prevail throughout the dynamics. The OD1 of Asp242 was found to make short hydrogen bonding contact with hydrogen of O3′ of pAPIRH$^+$ ($R_{O\cdots O}$= 2.5 ± 0.08 Å). The average bonding distances of pAPIRH$^+$ into the enzyme determined by molecular dynamics simulation are provided in Figure 4. The imino nitrogen (N4′) of pAPIRH$^+$ was found to be within 2.8 Å of OD1 of Asn168 in the X-ray structure. This hydrogen bond was present for 56% of time during the production phase of the dynamics ($R_{H\cdots O} \leq 2.0$ Å). The average distance between the OD1 of Asn168 and N4′ of pAPIRH$^+$ was found to be 2.9 ± 0.2 Å during E·pAPIRH$^+$ dynamics. The X-ray crystal structure of the D-subunit of the enzyme showed unusual near-eclipsed geometry for the bound inhibitor with the torsion angle (N4′−C4′−C5′−O5′) at 43° and the distance between N4′ and O5′ as 2.8 Å. A similar geometry is observed during the dynamics with dihedral angle (N4′−C4′−C5′−O5′) at 51 ± 12° (Figure 5A) and a distance N4′ to O5′ of 2.9 ± 0.1 Å (Figure 6A). A short hydrogen bond was observed between the OE2 of Glu166 and O5′ of pAPIRH$^+$ throughout the dynamics ($R_{H\cdots O} = 1.6 \pm 0.08$ Å, Figure 7A). The second hydrogen on the imino nitrogen (N4′) of pAPIRH$^+$ was found to be involved in a weak intramolecular hydrogen bond to O5′ of pAPIRH$^+$ ($R_{H\cdots O} = 2.5 \pm 0.2$ Å).

During the simulation, a hydrogen-bonding network (Figure 4) was observed between pAPIRH$^+$-O2′-Asp14-His241 triad. A hydrogen bond between the 2′-hydroxyl group and the OD1 of Asp14 was present for 98% of the observation time ($R_{H\cdots O} \leq 1.95$ Å, Figure 8A). The triad is completed by OD2 of Asp14 hydrogen bonding to Nδ of His241 for 97% of the observation time ($R_{H\cdots O} \leq 1.95$ Å, Figure 8B). During E·pAPIRH$^+$ dynamics, the activated nucleophilic water molecule (Wat138) was found to be oriented in a proper direction for attack at the ribosyl 1′-carbon of the inhibitor (3.2 ± 0.1 Å). This distance is in agreement with the suggested bond length of 3.1 Å between the oxygen of incipient water molecule and ribosyl 1′-carbon of transition state calculated from the kinetic isotope effects.[8] Fifteen percent of the time the distance was found to be 3.1 Å or less during the E·pAPIRH$^+$ dynamics. Wat138 appeared to make hydrogen bonds with OD2 of Asp10 and OD1 of Asn168 throughout SBMD1 dynamics. Fifteen percent of the time the hydrogen bond length between the OD2 of Asp10 and H1 of Wat138 was 1.65 Å or less.

Enzymatic Contacts with the Aromatic Ring of pAPIRH$^+$ in SBMD1. Residues 229−240 in the aromatic leaving-group pocket have high crystallographic *B*-factors and were found to be very flexible during the MD simulation. Large movements were observed in this pocket. There was a dramatic relocation in the position of Tyr229 during the simulation. It was found to hydrogen bond to the nitrogen attached to the aromatic ring (N29) for the first 320 ps, but apparently due to high flexibility of the loop containing this residue, the hydrogen bond broke after 320 ps. Residue movement was also observed for Phe167. During the dynamics Phe167 was found to make π−π stacking interaction with the aromatic ring of the inhibitor (Figure 9).
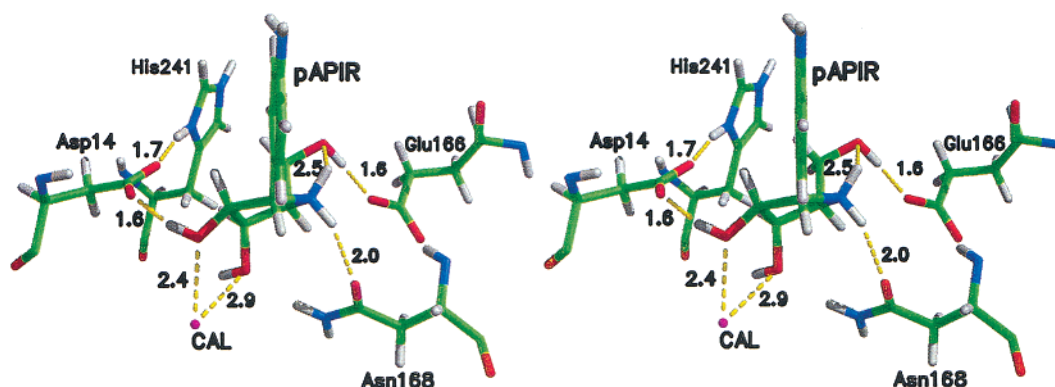
Figure 4. Stereoimage of the interactions of pAPIRH$^+$ with the active-site residues. Calcium is shown in magenta, hydrogen in white, carbon in green, oxygen in red, and nitrogen in blue.
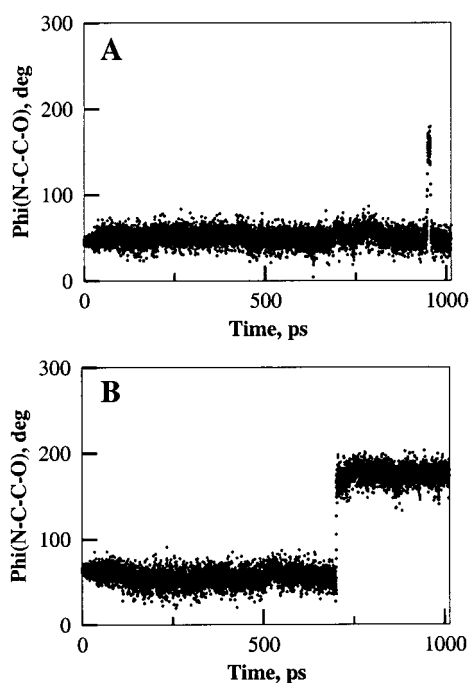

Figure 5. Conformation of the dihedral angle (N4′−C4′−C5′−O5′) in pAPIRH$^+$ (A) and pAPIR (B).

Figure 6. Distance between N4′ of and O5′ of inhibitor in pAPIRH$^+$ (A) and pAPIR (B).

Strong anticorrelated motion was observed between the residues 73−82 and 227−233 and between residues 227−233 and 159−160 (Figure 10), which are part of the substrate/inhibitor entry and leaving-group binding−activation region. Significant anticorrelated motion was also observed between the residues 141−147 and 73−82.

Enzymatic Contacts with the Iminoribitol Ring of pAPIR in SBMD2. The octacoordinated calcium was ligated by the amino acids, Thr126 (2.2 ± 0.7 Å), Asp242 (2.2 ± 0.7 Å), Asp15 (2.5 ± 0.17 Å; 2.2 ± 0.07 Å) and Asp10 (2.2 ± 0.07 Å). A comparison of the distance between all the ligands and calcium from our MD simulations (SBMD1 and SBMD2) and X-ray structure is presented in Table 1. Figure 11, based on E·pAPIR molecular dynamics simulation, shows various interactions of pAPIR in the active site. A hydrogen bonding interaction was observed between the neutral imino nitrogen (N4′) of pAPIR and Asn168 OD1 in E·pAPIR dynamics ($R_{\mathrm{H}\cdots\mathrm{O}} = 2.4 ± 0.3$ Å). The hydrogen bond between OD1 of Asn168 and imino nitrogen (N4′) in E·pAPIR dynamics was unstable compared to E·pAPIRH$^+$ dynamics. The average distance between the OD1 of Asn168 and N4′ of pAPIR was found to
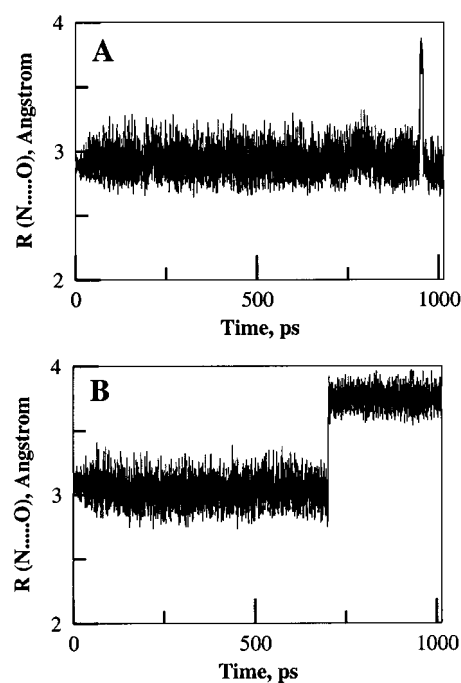
be 3.4 ± 0.3 Å during E·pAPIR dynamics. The distance between the hydrogen on N4′ and Asn168 OD1 was 2 Å or less in only 0.1% of the population. Large fluctuations were observed in the torsion angle N4′−C4′−C5′−O5′ (94 ± 54°, Figure 5B). The large fluctuation could be attributed to the absence of the hydrogen-bonding interaction between the N4′ and O5′. This is manifested in terms of rotation across the dihedral N4′−C4′−C5′−O5′ and an increase in distance between N4′ and O5′ (3.3 Å, Figure 6B). The hydrogen bond between OE2 of Glu166 and 5′-hydroxyl also terminated after 650 ps for the rest of the simulation ($R_{\mathrm{H}\cdots\mathrm{O}} = 2.3 ± 0.7$ Å, Figure 7B).

Table 1. Comparison of the Calcium Ion-ligand Coordination Structure in the X-ray (D-subunit), SBMD1 and SBMD2. Distances in Å

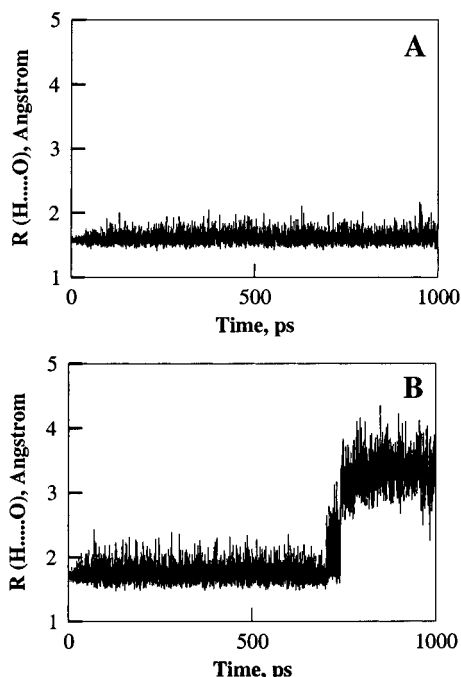|	X-ray	SBMD1	SBMD2
Asp10 OD1	2.5	2.20 ± 0.06	2.20 ± 0.07
Asp15 OD1	2.4	2.20 ± 0.07	2.20 ± 0.07
Asp15 OD2	2.6	2.30 ± 0.09	2.48 ± 0.17
Thr126 O	2.2	2.19 ± 0.06	2.22 ± 0.07
Asp242 OD2	2.5	2.17 ± 0.06	2.19 ± 0.07

Figure 7. Formation and breaking of hydrogen bond between hydrogen of inhibitor-O5′ and OE2 of Glu166 in pAPIRH$^+$ (A) and pAPIR (B).

The hydrogen-bonding network between pAPIRH$^+$-O2′-Asp14-His241 triad observed in case of E·pAPIRH$^+$ dynamics was also found to be present in E·pAPIR dynamics. The hydrogen bond between the 2′-hydroxyl group and OD1 of Asp14 was present for 96% of the observation time ($R_{H\cdots O}$ = 1.95 Å, Figure 8C). The hydrogen bond between OD2 of Asp14 and N-δ of His241 was present for 59% of observation time ($R_{H\cdots O}$ = 1.95 Å, Figure 8D). The average distance between OD2 of Asp14 and H-δ of His241 was found to be 2.0 ± 0.4 Å. The activated water nucleophile (Wat138) was found to be at a distance 3.2 ± 0.1 Å from the C1′ of the iminoribitol ring. Eighteen percent of the time this distance was less than 3.1 Å. The hydrogen bond between Wat138 and Asp10 was short and stable during the dynamics, as it was seen for the positively charged inhibitor.

Enzymatic Contacts with the Aromatic Ring of pAPIR. No strong hydrogen-bonding or hydrophobic interaction was observed for the aromatic ring of neutral pAPIR. Drastic movements of the loop 229−233 were observed during the dynamics. No hydrogen-bonding interaction between Tyr229 and nitrogen on the aromatic ring or π−π stacking of aromatic ring and Phe167 were observed during molecular dynamics simulation of E·pAPIR.

Results from ab Initio Calculations. Conformational search of neutral 2′,3′-dideoxyiminoribitol yielded three energy minima when the C4′−C5′−O5′−H bond was rotated (Table 2). The orientation with the hydroxyl group in the gauche$^-$ orientation was the global energy minimum because the hydroxyl hydrogen has a favorable interaction with the amine nitrogen in this structure. The two other orientations of the hydroxyl group were more than 2 kcal/mol above the gauche$^-$ structure and had different ring pucker angles. Moreover, upon introduction of the 3′-hydroxyl group, the two latter orientations became unstable. Optimization of the neutral 2′-deoxyiminoribitol and iminoribitol gave structures where the critical dihedral angle, O5′−C5′−C4′−N4′, differed significantly from the value

observed in the crystal structure of the enzyme-bound inhibitor (Table 2). Conformational search of the cationic 2′,3′-dideoxy-iminoribitol yielded only one stable orientation for the 5′-hydroxyl hydrogen. The hydroxyl group preferred an anti orientation as this geometry allowed a close interaction between the positively charged imino hydrogen and the 5′-hydroxyl oxygen. This electrostatic interaction is apparently responsible for the unusually small (about 42° in the crystal structure) dihedral angle between the hydroxyl group and the charged imino group. Optimizations of cationic 2′-deoxyiminoribitol and iminoribitol gave structures where this dihedral angle was very close to the average value as measured from the crystal structure of the bound inhibitor (Table 2).

Table 2. Comparison of Structures of Neutral and Protonated Model Compounds with the Crystal Structure of Bound *p*-Aminophenyliminoribitol; Selected Dihedral Angle Values Are Given in Degrees

crystal structure	HO–C$_5$C$_4$	OC$_5$–C$_4$N	C$_5$C$_4$–NC$_1$
	N/A	41.7	88.2
2′,3′-dideoxyiminoribitol			
neutral-g$^+$	66.3	65.2	169.5
neutral-g$^-$	−49.5	50.6	119.0
neutral-a	−167.0	66.3	167.8
cationic-a	174.8	42.3	109.6
2′-deoxyiminoribitol			
neutral-g$^-$g$^-$	−39.7	54.8	84.9
neutral-g$^-$a	−39.6	54.6	86.6
cationic-ag$^-$	170.5	45.0	80.8
cationic-aa	169.0	44.3	81.5
iminoribitol			
neutral-g$^-$a	−39.1	54.7	86.8
cationic-aa	167.6	43.7	80.1

Discussion

The mode of binding of the inhibitor *p*-aminophenyliminor-ibitol to nucleoside hydrolase has not been clearly defined by experimental work despite thorough kinetic and structural work.[10,12] The pH versus K_i profile shows that the neutral form of phenyliminoribitol inhibitor is captured from the solution, and analysis of the slow-onset component of inhibition suggests that protonation of the bound inhibitor might occur in the active site after the capture.[12] X-ray crystallography data does not reveal the position of hydrogen atoms, and the original interpretation of the electron density assumed that a neutral inhibitor resides in the active site.[10] By computer simulation techniques we have reinvestigated the question of whether the neutral or protonated form of the inhibitor is bound to the nucleoside hydrolase.

A visual comparison of the X-ray and the average simulated structures revealed a close match when the protonated inhibitor resides in the active site. Throughout the E·pAPIRH$^+$ dynamics (SBMD1), the inhibitor was bound in a stable manner to the active site. In contrast, the inhibitor in E·pAPIR dynamics (SBMD2) had a tendency to depart from calcium ligation. Ab initio calculations showed that the conformation of the proto-nated inhibitor is consistent with the crystallographic results, while the neutral inhibitor prefers a conformation that is different from the experimentally observed one. The pAPIRH$^+$ resembles the charge and geometry of the ribooxocarbenium ion transition state and can be looked upon as a transition-state analogue inhibitor. The resemblance of the E·pAPIRH$^+$ MD simulated
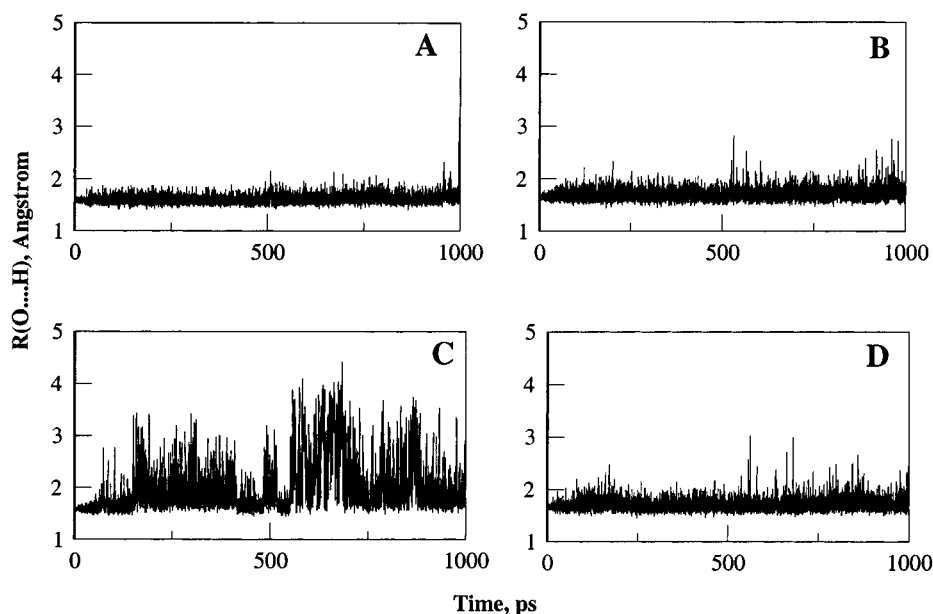
Figure 8. Histograms for the hydrogen bonding triad, pAPIRH$^+$-O2′-Asp14-His241. **(A)** Hydrogen-bonding interaction between the OD1 of Asp14 and 2′-hydroxyl group of pAPIRH$^+$. **(B)** Distance between OD2 of Asp14 and Nδ of His241 in pAPIRH$^+$. **(C)** Hydrogen-bonding interaction between the OD1 of Asp14 and 2′-hydroxyl group of pAPIR. **(D)** Distance between OD2 of Asp14 and Nδ of His241 in pAPIR.
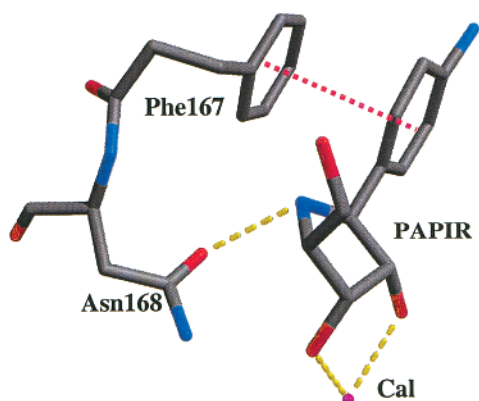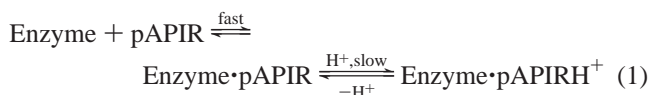

Figure 9. Snapshot from E·pAPIRH$^+$ dynamics (SBMD1). $\pi-\pi$ stacking interaction between the aromatic ring of Phe167 and pAPIRH$^+$.

structure and the X-ray structure of the enzyme−inhibitor strongly supports a two-step mechanism (eq 1), wherein the imino nitrogen picks up a proton in the second step of inhibition, yielding a tightly bound pAPIRH$^+$:

$$\text{Enzyme} + \text{pAPIR} \underset{}{\overset{fast}{\rightleftharpoons}}$$
$$\text{Enzyme·pAPIR} \underset{-H^+}{\overset{H^+, slow}{\rightleftharpoons}} \text{Enzyme·pAPIRH}^+ \quad (1)$$

The hydrogen bond between the imino nitrogen (N4′) of pAPIRH$^+$ and Asn168 OD1 was more populated in SBMD1 (56%) as compared to SBMD2 (0.1%). This hydrogen bond might be an important feature for the stabilization of pAPIRH$^+$ over pAPIR.

The X-ray structure of the enzyme−inhibitor complex reveals an unusual orientation of the 5′-hydroxyl group with respect to the iminoribitol ring of the inhibitor. The torsion angle N4′−C4′−C5′−O5′ of the enzyme-bound inhibitor was near 42°, bringing N4′ at a distance 2.7 Å from O5′ of the inhibitor. Such interaction has been proposed to stabilize the transition-state oxocarbenium ion via the neighboring-group interaction of the
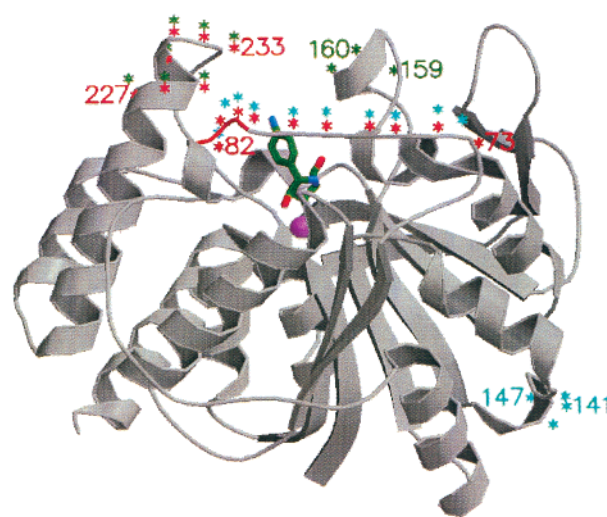

Figure 10. Negative correlated motions observed during production phase of E·pAPIRH$^+$ dynamics. Residues, which display strong negative correlated motion, are marked with similarly colored stars. For example, residues 227−233 and 82−73 show anti correlated motion and are marked with red stars. Residues without any stars do not show any significant anti correlated motion. Calcium is shown in magenta and inhibitor in green. Plot generated with program MOLSCRIPT.[28]

lone pair electrons from O5′.[11,23] Two possible forces can restrain the inhibitor in that particular unusual conformation: (i) influence of the local environment in the enzyme−formation of the short hydrogen bond between Glu166 and 5′-hydroxyl forces it to occupy syn geometry and (ii) intramolecular hydrogen bond−weak hydrogen-bonding interaction by the hydrogen on the imino nitrogen and 5′-hydroxyl group. The conformation of the iminoribitol ring of the inhibitor in E·pAPIRH$^+$ dynamics closely resembles the X-ray crystal structure of the inhibitor in the enzyme−inhibitor complex. The weak hydrogen-bonding interaction between the imino nitrogen (N4′) and O5′ in the neutral inhibitor was absent during SBMD2

(23) Horenstein, B. A.; Schramm, V. L. *Biochemistry* **1993**, *32*, 7089.
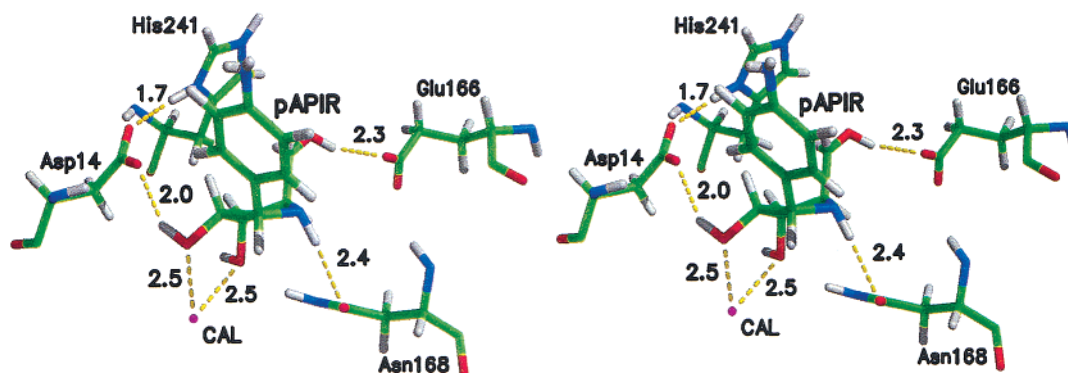
Figure 11. Stereoimage of the interactions of pAPIR with the active-site residues. Calcium is shown in magenta, hydrogen in white, carbon in green, oxygen in red, and nitrogen in blue.

dynamics because the hydrogen on the imino nitrogen (N4′) of the inhibitor pointed toward Asn168 OD1. This might be one of the possible reasons for the structural fluctuations around the N4′−C4′−C5′−O5′ dihedral and collapse of the unusual geometry of the inhibitor in E·pAPIR dynamics.

The high population of the hydrogen bonds in pAPIRH$^+$-O2′-Asp14-His241 triad suggests the requirement of the observed hydrogen-bonding network pattern for the stabilization of the E·pAPIRH$^+$ complex in SBMD1. Although the hydrogen-bonding network exists in the case of E·pAPIR dynamics, the interaction between the O2′ hydroxyl and Asp14 OD1 (59%) was less populated compared to that in E·pAPIRH$^+$ dynamics (97%). Studies have shown that mutation of His241 to Ala results in a 1000-fold decrease of the rate of reaction.[4] Examination of Figure 2 shows that His241 of the triad though hydrogen-bonded to Asp14 can still be in the vicinity of the aromatic ring of pAPIRH$^+$. The presence of the hydrogen-bonding network (pAPIRH$^+$−O2′···Asp10···His241) that was observed in molecular dynamics simulation (SBMD1) makes His241 more positively charged; thus, the latter may become a better protonating agent for the leaving nucleobase. It is widely appreciated that K_{app} values determined from the pH rate profiles reflect combinations of K_a values and kinetic constants.[24] The dependence of rate upon pH for the enzymatic reaction established is most simplistically interpreted as being dependent upon a group with pK_{app} of 9.1, which must be protonated, and a group with pK_{app} of 7.1, which must be unprotonated.[12] Mutagenesis and substrate specificity studies have implicated His241 to be the group associated with pK_{app} 9.1.[4] The unprotonated group associated with pK_{app} 7.1 has been suggested as one of the active-site carboxylates.[12] The high population of the short hydrogen bond between OD1 of Asp 10 and Wat138 in SBMD1 suggests a possibility of Asp10 as the group with pK_{app} 7.1 that is needed only for catalytic activity and not binding. Aspartates with unusually high pK_a have been reported earlier in the literature.[25,26]

The enzymatic residues of the leaving-group pocket were found to be flexible during both MD simulations (E·pAPIRH$^+$ and E·pAPIR). One of the functions for this flexibility might be to accommodate nucleobases, inosine and uridine, which themselves have a large difference in size. The residues of the

leaving-group pocket appeared to stabilize the aromatic ring in the case of SBMD1. Unlike the many close hydrogen-bonding interactions surrounding the iminoribitol ring, the aromatic ring contacts were mainly hydrophobic in E·pAPIRH$^+$ dynamics. Phe167 was observed to form a π−π stacking interaction with the aromatic ring of the inhibitor in E·pAPIRH$^+$ dynamics. No such interaction was observed for E·pAPIR dynamics. This kind of π−π stacking interaction has been found in DNA binding enzymes.[27] Although this was not observed in the X-ray structure, it is an expected interaction and contributes to inhibitor binding to the hydrophobic pocket. Prior experiments have shown that among all the known inhibitors of IU-NH, the compounds that have a hydrophobic phenyl ring substituent at the ribose C1′ bind the enzyme more strongly.[9] Thus, the π−π stacking interaction strengthens the binding of pAPIRH$^+$. Horenstein and Schramm have shown that the hydrophobic leaving-group effect is enhanced by the affinity of the phenyl group substituent and accounts for a 15-fold more rapid equilibrium binding of inhibitor compared to that of the unsubstituted iminoribitol but slows the onset to the second phase (eq 1) of inhibition.[11] The binding energy of iminoribitol inhibitors with phenyl substituent is approximately −5 kcal/mol more favorable than that of the substrate inosine.[9] The following interactions between pAPIRH$^+$ and IU-NH were found to be present during the dynamics, which can account for this favorable binding by −5 kcal/mol: (i) a hydrogen bond between OD1 of Asn168 and N4′ of pAPIRH$^+$, (ii) a weak bond between hydrogen on imino nitrogen (N4′) and O5′ of pAPIRH$^+$, and (iii) a π−π hydrophobic interaction between the aromatic rings of Phe167 and pAPIRH$^+$.

Strong anticorrelated motion between the residues 73−82 and 227−233 and between residues 227−233 and 159−160 (Figure 10) are important since these residues belong to the substrate/inhibitor entry- and leaving-group binding−activation region. Significant long-distance anticorrelated motion between the residues 141−147 and "active-site loop" 73−82 were observed during the production phase although these residues were approximately 32 Å from each other. Since the inhibitor resembles the TS somewhat, it is possible that these motions would also be found in E·TS.

(24) Bruice, T. C.; Schmir, G. L. *J. Am. Chem. Soc.* **1959**, *81*, 4552.
(25) Andersen, J. F.; Sanders, D. A. R.; Gasdaska, J. R.; Weichsel, A.; Powis, G.; Montfort, W. R. *Biochemistry* **1997**, *36*, 13979.
(26) Adams, J.; Johnson, K.; Matthews, R. T.; Benkovic, S. J. *Biochemistry* **1989**, *28*, 6611.

(27) Eads, J. C.; Scapin, G.; Xu, Y.; Grubmeyer, C.; Sacchettini, J. C. *Cell* **1994**, *78*, 325.
(28) Kraulis, P. J. *J. Appl. Crystallogr.* **1991**, *24*, 945.

Conclusions

Ab initio calculations and molecular dynamics simulations have been used to determine the protonation state of the inhibitor *p*-aminophenyliminoribitol in the active site of nucleoside hydrolase from *Crithidia fasciculata*. Structure minimization at the MP2/6-311+G(d,p) level showed that only the protonated form of the inhibitor is consistent with the crystallographic data. Molecular dynamic simulations of protonated pAPIRH$^+$ (SB-MD1) and neutral pAPIR (SBMD2) bound at the active site of nucleoside hydrolase show that the positively charged species is bound most tightly. Overall, the structure of E·pAPIRH$^+$ determined by MD simulation is in an excellent agreement with the three-dimensional X-ray structure. The molecular dynamics simulated structures for enzyme-bound neutral inhibitor differ significantly from the X-ray structure. The pH dependence of inhibitor binding suggests that the neutral species is first bound to the active site of IU-NH followed by a structural change and protonation (eq 1). Wat138 is present at a close proximity to the C1′ of the ribose ring throughout the SBMD1 such that it likely represents the nucleophilic water in reaction of enzyme and substrate. Asp10 can be the group with pK_a 7.1, which needs to be in the unprotonated form for the catalysis because it is crucial for the polarization of the nucleophilic water but not for the binding of the substrate. The aromatic side chain of pAPIRH$^+$ nestles into a hydrophobic side pocket in the active-site tunnel, which serves as an anchor for the C1′ aniline substituent. The $\pi-\pi$ stacking interaction between the rings of Phe167 and pAPIRH$^+$ aromatic ring is present in E·pAPIRH$^+$ but not in E·pAPIR dynamics. The π-stacking interaction might be one of the reasons for high affinity binding of pAPIRH$^+$ inhibitor. The hydrogen bond between imino nitrogen and Asn168 oxygen was present for 56% of time in SBMD1 (E·pAPIRH$^+$) and 0.1% time in SBMD2 (Enzyme·pAPIR). The distance of the imino nitrogen to the 5′-oxygen of the iminor-ibitol ring was stabilized at 2.9 Å for SBMD1, which may be compared to 3.7 Å in SBMD2. Because the active site is lined with negatively charged residues, it is expected that a positively charged inhibitor, similar to the ribooxocarbenium ion TS, will be more stabilized than a neutral form. Thus, the pAPIRH$^+$ species of the inhibitor warrants classification as a transition-state inhibitor.[11] Observed deviations of ±0.3 Å from the X-ray structure for the calcium and its ligands can be due to the lack of polarization in the CHARMM force field. In the current simulation, we have corrected some partial charges to account for the induced polarization in the presence of calcium. Such small structural deviations are localized only to the nearest calcium ion neighbors.